Arab J. Nucl. Sci. Appl., Vol. 57, 2, 31-38 (2024)

ISSN 1110-0451

Arab Journal of Nuclear Sciences and Applications

Web site: ajnsa.journals.ekb.eg

(E S N S A)

Extension of Phase Variation, Higher Momentum Transfer Components and Pauli Blocking Effects on Reaction Cross Sections to Lower and Medium Energies

M.M. Taha and S. Esmail

Mathematics and Theoretical Physics Department, Nuclear Research Center, *Egyptian Atomic Energy Authority, Cairo, Egypt.*

ARTICLE INFO

Article history:

Received: 29th Nov. 2023

Accepted: 26th Dec. 2023

Available online: 10th Mar. 2024

Keywords:

Nuclear Reaction;
Reaction Cross Section;
Glauber Model.

ABSTRACT

The nucleus-nucleus total reaction cross section at 30-1000 MeV/n is studied, using a modified Coulomb Glauber model, which includes combined effects due to phase variation, higher momentum transfer components, Pauli blocking, and a finite range. The total reaction cross sections of the reactions: $^{12}C + ^{12}C$, $^{4}He + ^{16}O$, $^{20}Ne + ^{12}C$, $^{8}Li + ^{9}Be$, $^{8}Li + ^{12}C$ and $^{8}Li + ^{27}Al$ using different densities of the harmonic oscillator single-particle wave function (SDHO) are calculated and compared with the available experimental data and previous calculations. Using a simulated search program, the phase variation γ_{NN} parameter is treated as a free parameter to fit the experimental data of the reaction cross section σ_R. A good agreement with the experimental data is obtained. The relationship between the phase variation and finite range parameters as a function of incident energy is discussed. We investigated combined effects on p - ^{16}O reaction cross sections and compared with the available experimental data and previous calculations.

1 - INTRODUCTION

The basic nucleus-nucleus interaction [1] is described by the Glauber model [2] in terms of nucleon-nucleon interaction and nuclear properties. It is assumed that the nucleus moves in a straight path. This estimate is excellent at high energies. Due to Coulomb repulsion, the nucleus is diverted from a straight path at low energies. Heavy ion scattering at low energies is also extremely well described by the so-called coulomb modified Glauber model (CMGM) [3, 4, 5, 6]. The optical model approximation [7, 8, 9], with Coulomb and medium corrections provides an effective formula of nucleus-nucleus reaction cross section which is dependent on the nucleon-nucleon cross section (NNCS) and the nuclear densities. A lot of data regarding the structure of unstable nuclei [10, 11, 12, 13] using this approach.

One of the main issues in nuclear physics is the determination of density distributions, which is regarded as a key instrument in the analysis of nucleus-nucleus interactions [1, 14, 15]. The examination of the fundamental interactions between nuclei makes use of two different forms of density distributions: charge and matter distributions. Whereas the charge distribution very precisely predicted by distribution of protons [16], the matter distribution deals with the composition (p,n, pi-mesons, fields and so on) of neutrons and protons [17]. High-energy electron scattering and muonic X-rays are two techniques used to determine the nuclear charge distribution. Moreover, investigations involving Rutherford scattering, pionic X-rays, proton elastic scattering, and alpha decay can be used to reveal details regarding the distributions of nuclear materials. A variety of density distributions is including the harmonic oscillator density distribution [18, 19].

Ismail et al [20] calculated the reaction cross section of the reaction $^{12}C+^{12}C$ using the optical limit of the Glauber theory where the finite range and in-medium NN cross section σ_{NN} with appropriate density dependency were considered. The rms matter radii of ^{12}C nuclei have values 2.32 and 2.45 fm. They showed that smaller rms radius (2.32 fm) of the ^{12}C nucleus fits satisfactorily the experimental σ_R values, assuming a finite range NN interaction with β_{NN} = 1 fm^2.

Corresponding author: mahmoudmt@hotmail.com

DOI: 10.21608/ajnsa.2024.251756.1796

By using this method, Sharma et al. [21] investigated how much the reaction cross section varies on the target and projectile densities. They employed the densities from both spherically (Sph.) symmetric RMF theory and axially deformed (Def.) RMF theory. Additionally, they compare the outcomes derived from non-relativistic HF(SEI-I) densities and relativistic mean field densities. The result of spherical RMF(NL3) was in good agreement with the experimental results.

Abu-Ibrahim [22] had been found a (semi-empirical) relation for estimating nucleus-nucleus total reaction cross sections which requires the number of protons, the number of neutrons and the total cross sections of proton-proton and proton-neutron reactions. This expression is applicable in the energy range from 30A MeV to about 1A GeV

Ahmed et al [18] described the reaction cross sections of Oxygen isotopes at 1 Gev/u, using a modified Glauber amplitude, which considered corrections due to phase variation, higher momentum transfer, Pauli blocking and finite range, using SDHO density. They extended these effects to energy domain 650-1000 MeV/n.

The aim of the present work is to extend the combined effects of phase variation, higher momentum transfer components, Pauli blocking, and finite range of NN interactions amplitude to lower and intermediate energies. The total reaction cross sections of ^{12}C+^{12}C, ^{4}He+ ^{16}O, ^{20}Ne+ ^{12}C, ^{8}Li+ ^{9}Be, ^{8}Li+ ^{12}C and ^{8}Li+ ^{27}Al are calculated at 30-1000 MeV/n, using SDHO densities. Sec. 2 presents the mathematical model and the results are discussed in Sec. 3.

2. MATHEMATICAL MODEL

The nucleus-nucleus reaction cross section in the optical model can be written as [7, 8],

$$\sigma_R = 2\pi \int_0^\infty b\, db\, (1 - |S(b)|^2), \qquad (\mathbf{1})$$

where b is an impact parameter. In the optical limit approximation, the scattering matrix can be expressed in terms of the phase shift χ(b) as,

$$S(b) = e^{-i\,\chi(b)} \qquad (\mathbf{2})$$

where, $\chi(b)$ is the phase shift function, which can be written as [20].

$$\chi(b) = \frac{\sigma_{NN}}{k} \int_0^\infty q\, dq\, J_0(bq\, b)\;\; \tilde{\rho}_T(q)\tilde{\rho}_P(-q)\, f_{NN}(q) \quad (\mathbf{3})$$

where k is the incident nucleon momentum corresponding to the projectile kinetic energy per nucleon and q is the momentum transfer. Here, $\tilde{\rho}_T(q)$ and $\tilde{\rho}_P(-q)$ are the Fourier transforms of the nuclear densities of target and projectile and $J_0(bq\, b)$ is the cylindrical Bessel function of zeroth order. $f_{NN}(q)$, given higher momentum transfer components, can be written as [18, 19]

$$f_{NN}(q) = \left(\frac{i\,k}{4\,\pi} \sum_{n=0}^{\infty} A_{n+1} \left(\frac{\sigma_{NN}}{4\,\pi\,\beta_{NN}}\right)^n \frac{(1 - i\,\epsilon_{NN})^{n+1}}{n+1}\;\; e^{\frac{-\beta_{NN} q^2}{2\,(n+1)}}\right) e^{\frac{-i\,\gamma_{NN} q^2}{2}} \qquad (\mathbf{4})$$

where

$$A_{n+1} = \frac{A_1}{n(n+1)} + \frac{A_2}{(n-1)n} + \frac{A_3}{(n-2)(n-1)} + \cdots + \frac{A_n}{1 \times 2} \qquad (\mathbf{5})$$

with $A_1 = 1$. ϵ_{NN} , β_{NN} and γ_{NN} are the ratio of the real to imaginary parts of the forward NN amplitude, the finite range parameter and the phase variation respectively.

The NN total cross section is given by

$$\sigma_{NN} = \frac{N_T\, N_P\, \sigma_{nn} + Z_T\, Z_P\, \sigma_{pp} + N_T\, Z_P\, \sigma_{np} + N_P\, Z_T\, \sigma_{np}}{A_T\, A_P} \qquad (\mathbf{6})$$

where, $Z_{T(P)}$, $N_{T(P)}$ and $A_{T(P)}$ are the proton, neutron and mass of the target (projectile) nucleus. The NN cross-section σ_{ii}, (ii = pp, np, nn), we used the parametrization of which fit NN scattering data from 10-1000 MeV by phenomenological formula for in-medium nucleon-nucleon cross section is proposed by the following expression [23]:

$$\sigma_{pp} = (13.73 - 15.04(v/c)^{-1} \;+\; 8.76\,(v/c)^{-2} + 68.67\;(v/c)^4)\frac{1 + 7.772\,E_{lab}^{0.06}\;\rho^{1.48}}{1 + 18.01\,\rho^{1.46}} \qquad (\mathbf{7})$$

$$\sigma_{np} = (-70.67 - 18.18(v/c)^{-1} \;+\; 25.26\,(v/c)^{-2} + 113.85\,(v/c))\frac{1 + 20.88\,E_{lab}^{0.04}\;\rho^{2.02}}{1 + 35.86\,\rho^{1.9}} \qquad (\mathbf{8})$$

$$\sigma_{pp} = \sigma_{nn} \qquad (\mathbf{9})$$

where, the velocity $\frac{v}{c} = \sqrt{1 - \frac{1}{\gamma^2}}$, $\gamma = \frac{E_{lab}}{931.5} + 1$ and ρ is the total nuclear density. We take the average nuclear density of $\rho = \rho_0$ [29], where $\rho_0 = 0.17$ fm^{-3}.

In the presence of Coulomb field, the trajectory deviates from the field-free straight line trajectory and the function χ(b) is overestimated. To correct for this, it was suggested in Ref [5] the trajectory to be a straight line at $\grave{b}$, the distance of closet approach instead of at b as discussed in Ref [5, 6] which is the distance of the closest approach in Rutherford oribts. The quantity $\grave{b}$ is given in terms of k and the Sommerfeld parameter η as

$$k\,\acute{b} = \eta + \sqrt{(\eta^2 + k^2 b^2)} \qquad (\mathbf{10})$$

with, $\eta = \frac{Z_P\, Z_T\, e^2}{\hbar\, v}$, where v is the projectile-target relative velocity.

The proton and neutron densities distributions of nuclei using the Slater determined constructed from the harmonic oscillator single particle wave functions SDHO expressions are given by means of the equations shown by [18, 19]

$$\rho_n = n\,\rho_0(r), \qquad n = 1,2 \qquad (\mathbf{11})$$

$$\rho_n = \rho_2(r) + (n-2)\left[1 - \frac{1}{4\,\alpha^2 p^2} + \frac{r^2}{24\,\alpha^2 p^4}\right]\rho_0, \qquad n = 3,\ldots,8, \qquad (\mathbf{12})$$

$$\rho_n = \rho_8(r) + (n-8)\left[1 - \frac{1}{2\,\alpha^2 p^2} + \frac{1}{16\,\alpha^4 p^4} + \left(\frac{1}{12\,\alpha^2 p^4} - \frac{1}{48\,\alpha^4 p^6}\right) r^2 + \frac{r^4}{960\alpha^4 p^8}\right]\rho_0, \qquad n = 9,\ldots,14, \qquad (\mathbf{13})$$

where

$$\rho_0(r) = \frac{1}{8\,\pi^{3/2}}\, e^{\left(-\frac{r^2}{4p^2}\right)}, \qquad p^2 = \frac{A-1}{4\alpha^2\, A}, \qquad (\mathbf{14})$$

and n is the number of protons/neutrons in the given nucleus. The quantities α^2 and A in the above equations are the oscillator constant and number of nucleons in the nucleus, respectively.

3. RESULTS AND DISCUSSION

The nucleon-nucleon cross section [24] is considered one of the main components of the nuclear transport theory. Numerous studies have examined the nucleon-nucleon cross section's in-medium effects [25, 26, 27, 28], taking into account its dependence on nuclear matter density and incoming energy. The σ_R computations are greatly improved by these investigations. The current experimental results and model predictions, however, nevertheless occasionally disagree in a variety of incidence energies and reaction systems [23]. The nuclear density distributions and nucleon-nucleon cross section are not sufficient to determine the σ_R calculations in-medium. Therefore, we adopt the method of Franco and Yin [29] to account for the phase variation impact. This method involves treating the phase γ_{NN} as a free parameter and increasing the NN amplitude Eq. (4) by the phase factor $e^{\frac{-i\,\gamma_{NN} q^2}{2}}$. In addition, we investigated the NN amplitude's higher momentum transfer components and took the following NN amplitude parametrization into consideration [30].

Table (1): The parameters of the σ_{NN} , ϵ_{NN} , β_{NN} , and γ_{NN} as a function of energy, E_{lab}

E_{lab} MeV/n	σ_{pp} fm²	σ_{pn} fm²	ϵ_{pp}	ϵ_{pn}	β_{pp} fm²	β_{pn} fm²	γ_{NN} fm²
30	6.89	22.014	1.29	0.4219	0.563	0.6535	0.2476
40	5.05	15.786	1.4655	0.673	0.728	0.817	0.1905
50	3.99	12.166	1.816	0.8648	0.8093	0.959	0.1004
60	3.32	9.83	1.899	1.072	0.8371	0.995	0.096
70	2.859	8.227	1.983	1.28	0.859	1.032	0.059
80	2.532	7.066	1.74	1.03	0.85	0.85	-0.015
100	2.12	5.53	1.87	1.0	0.66	0.36	0.4125
150	1.694	3.767	1.53	0.96	0.57	0.58	0.177
200	1.62	3.099	1.15	0.71	0.56	0.68	-0.015
325	1.88	2.692	0.45	0.16	0.26	0.36	-0.46
425	2.21	2.716	0.47	0.25	0.21	0.27	-0.421
650	2.93	2.94	-0.5119	-0.5832	0.252	0.2492	0.0895
800	3.35	3.092	-0.5181	-0.5900	0.2539	0.2602	0.0545
1000	3.80	3.25	-0.2373	-0.5932	0.1216	0.2582	0.2292

The value of the parameter σ_{NN} is determined by Eqs. (6-9). We use the average nuclear densities of $\rho = \rho_0 = 0.17$ for energies between 30 and 1000 MeV/n [31]. The finite range parameter β_{NN} and the ratio of the real to imaginary parts ϵ_{NN} are taken to be energy-dependent. The energy range from 30 to 70 MeV is taken from Ref. [32], and for 100 to 550 MeV is considered from Ref. [33], while for E_{lab} =650, 800 and 1000 are determined from Ref. [34]. The phase variation γ_{NN} parameter is treated as a free parameter. The corresponding parameters of the pp and pn amplitudes are listed in Table 1.

The calculated $^{12}C+^{12}C$ total reaction cross section at 30-1000 MeV/n using the modified Coulomb Glauber model is shown in Fig. 1 with a comparison between experimental data [35, 36] and previous calculations [20, 21, 22]. Fig. 1 shows that the present calculations which consider the combined effects of Pauli blocking, finite range, higher momentum transfer components, and phase variation (solid line) give better agreement with recent data [35] than the previous calculations of [20, 21, 22], which neglected combined effects.

The nuclear density distributions are calculated using the SDHO expressions along with the oscillator constant set [18, 19] (see Eqs. 11-14) which is the ground state density. For, the oscillator constants for proton and neutron distributions α_p^2 and α_n^2 respectively, we assumed equal values of α_p^2 and α_n^2 for the $N = Z$. The values α_p^2 and α_n^2 are obtained from proton $\langle r_p^2\rangle^{1/2}$ and neutron $\langle r_n^2\rangle^{1/2}$ rms radii [37] are listed in table 2. The values $\langle r_p^2\rangle^{1/2}$, $\langle r_n^2\rangle^{1/2}$ and matter $\langle r_m^2\rangle^{1/2}$ of ^{12}C, ^{16}O are taken from Ref. [37], ^{4}He from Ref. [38], ^{20}Ne from Ref. [39], ^{8}Li and ^{9}Be from Ref. [40] and ^{27}Al from Ref. [41].

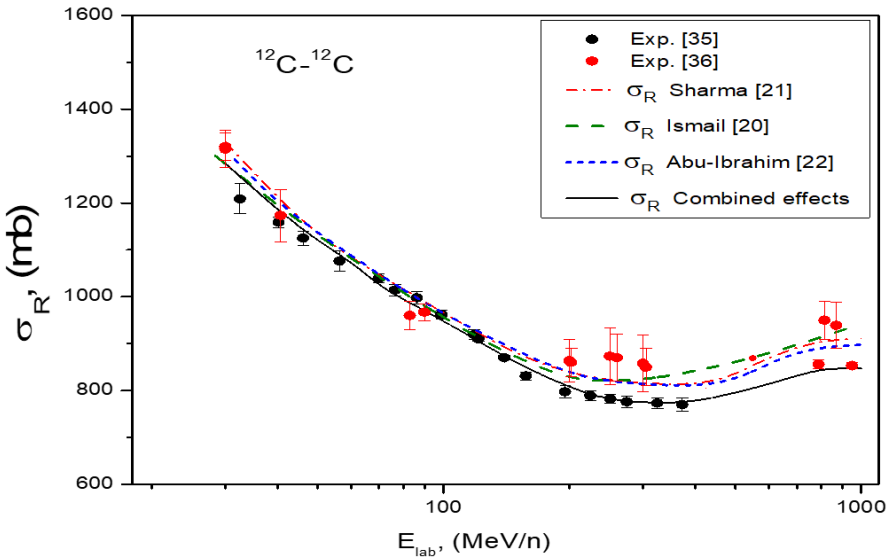

Fig. (1): The calculated $^{12}C+^{12}C$ total reaction cross section at 30-1000 MeV/n using CMGM which consider the combined effects is shown, along with comparisons with experimental data and previous calculations.

Table (2): The values $\langle r_p^2\rangle^{1/2}$, $\langle r_n^2\rangle^{1/2}$ and $\langle r_m^2\rangle^{1/2}$and the values the oscillator constant α_p^2 and α_n^2

Nucleus		$\langle r_n^2\rangle^{1/2}$ fm	$\langle r_p^2\rangle^{1/2}$ fm	$\langle r_m^2\rangle^{1/2}$ fm	α_p^2	α_n^2
^{12}C	[37]	2.31	2.33	2.32	0.3760	0.3826
^{16}O	[37]	2.54	2.54	2.54	0.3342	0.3342
^{4}He	[38]	1.57	1.57	1.57	0.4564	0.4564
^{20}Ne	[39]	2.8008	2.835	2.8179	0.3091	0.3017
^{8}Li	[40]	2.802	2.17	2.583	0.2436	0.3495
^{9}Be	[40]	2.67	2.35	2.53	0.2710	0.3320
^{27}Al	[41]	3.03	3.03	3.03	0.2183	0.2077

In Figs. 2, 3, we applied the combined effects for calculation of the total reaction cross section for the systems: ^{4}He+ ^{16}O, ^{20}Ne+^{12}C, ^{8}Li+ ^{9}Be, ^{8}Li+ ^{12}C, and ^{8}Li+ ^{27}Al. These Figs. show that the combined effects are in good agreement with experimental data in all systems. The experimental data are taken from ^{4}He+ ^{16}O [42, 43], ^{20}Ne+ ^{12}C [36, 44], ^{8}Li+ ^{9}Be [45], ^{8}Li+ ^{12}C [45], and ^{8}Li+ ^{27}Al [45].

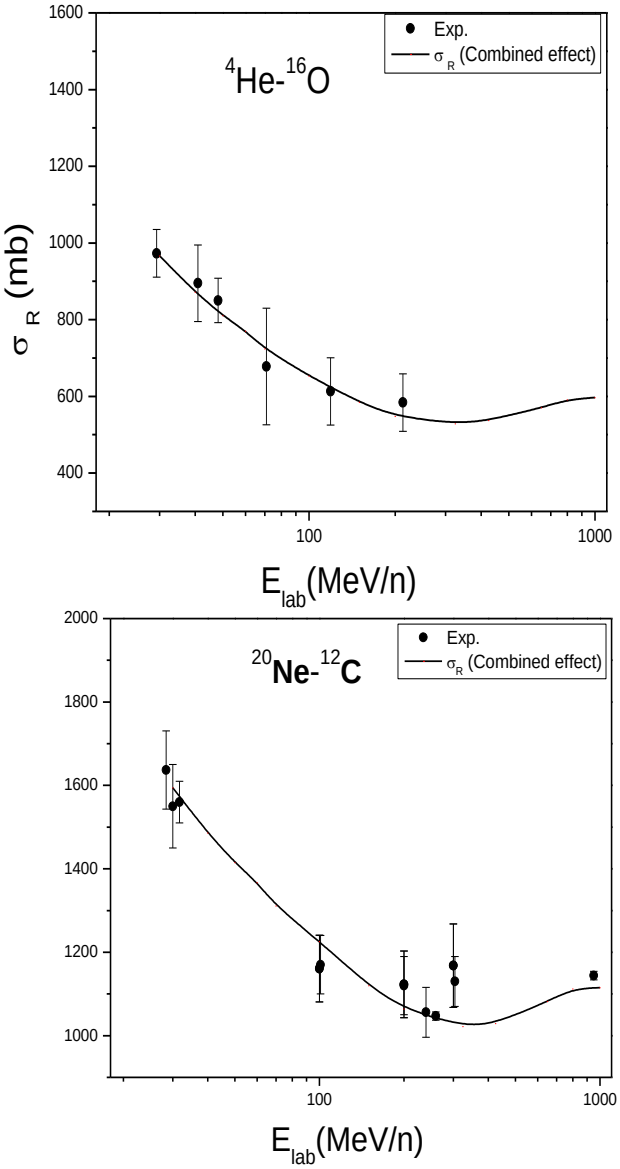

Fig. (2): The total nuclear reaction cross-section σ_R using MCGM con- siders the combined effects for two systems ^{4}He+ ^{16}O and ^{20}Ne+ ^{12}C as a function of the energy of the projectile per nucleon.

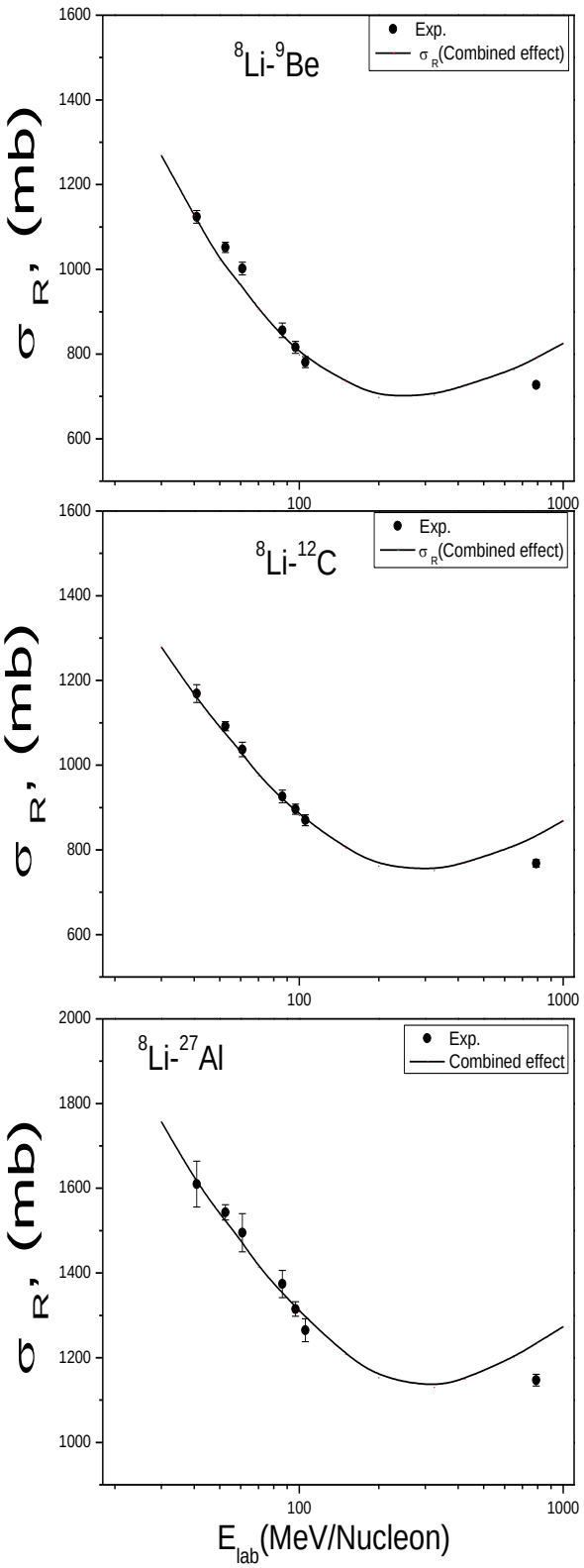

Fig. (3): The same Fig. 2 but for the systems, ^{8}Li+ ^{9}Be, ^{8}Li+ ^{12}C, and ^{8}Li+ ^{27}Al.

Figure 4 indicates the different values of γ, which reproduce the best values of σ_R, and the finite range parameter as a function of incident energy per nucleon. From these two curves, it is clear that the curve of phase variation decreases until it reaches the minimum point at E_{lab} = 65 MeV, then increases to be a maximum at E_{lab} = 115 MeV, then reaches the absolute minimum at E_{lab} = 375 MeV. While the finite range β_{NN} has opposite behavior, it increases until it reaches its maximum point at E_{lab}= 65 MeV, then reaches its minimum at E_{lab} = 115 MeV. After E_{lab}= 375 MeV, there are no dramatic changes in the values of β_{NN} as the energy increases up to 1000 MeV.

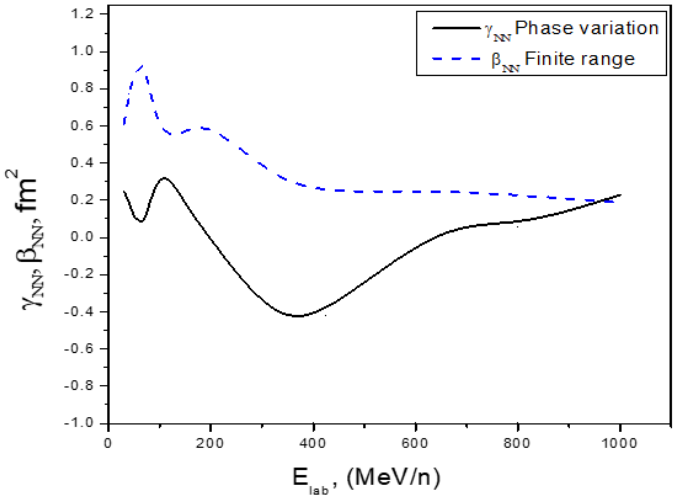

Fig. (4): The different values of parameters, the phase variation γ_{NN} , and the finite range β_{NN} as a function of incident energy per nucleon.

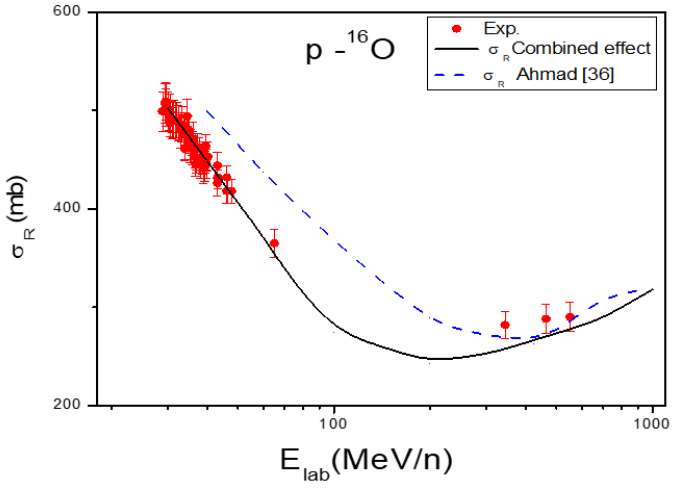

Fig. (5): Reaction cross sections of p-^{16}O in the energy range 30-1000 MeV/n. The solid and dashed lines represent the results using the combined effect and Ahmad calculation's, respectively.

Figure 5 shows the total reaction cross sections of p-^{16}O in the energy range 30-1000 MeV/n using CMGM, which including combined effects (solid line). We compared with Ahmad et al. [18] (dashed line), who also used SDHO densities but without including combined effects. The present work gives better agreement with experimental data than Ahmad et al. [18] calculations at low and intermediate energies, which shows the importance of combined effects. The experimental data are taken from Carlson [46].

REFERENCES

[1] P.J. Karol, (1975) Nucleus-nucleus reaction cross sections at high energies: Soft-spheres model, Phys. Rev. C 11, 1203-1209.

[2] R. J. Glauber, Lectures on Theoretical Physics, edited by W. E. Britton and L. G. Dunham (Wiley, New York, 1959), Vol. 1,p. 315.

[3] A. Vitturi and F. Zardi, (1987), Modified Glauber model for the description of elastic scattering between heavy ions, Phys. Rev. C 36, 1404-1407.

[4] I. Ahmad, M. A. Abdulmomen, and M. S. Al-Enazi, (2002) ^{12}C–^{12}C elastic scattering at intermediate energies, Phys. Rev. C 65, 054607.

[5] S.K. Charagi and S.K. Gupta, (1990) Coulomb-modified Glauber model description of heavy-ion reaction cross sections, Phys. Rev. C 41, 1610-1618.

[6] S.K. Charagi and S.K. Gupta, (1992) Coulomb-modified Glauber model description of heavy-ion elastic scattering at low energies, Phys. Rev. C 46, 1982-1987.

[7] Ibrahim M.A. Tag El-Din, M.M. Taha and Samia S.A. Hassan, (2014) Study of p-4He total reaction cross-section using Glauber and Coulomb-modified Glauber models, *Int. J. Mod. Phys.* E 23, 1450010.

[8] M.M. Taha and M. Rashdan, (2021) The effects of finite range of the NN force and in-medium NN cross-section on the proton–nucleus total reaction cross-section, Nucl. Inst. and Meth. in Phys. Rese. B 26 500-501.

[9] M.Rashdan, *M. M. Taha, T. A. Abdel-Karim and S. Esmail*, (2019), Analysis of the reaction cross-sections of $^{22-36}$Na + ^{12}C and $^{19-27}$F+ ^{12}C at 240 MeV/u, *Int. J. Mod. Phys.* E 28, 1950046.

[10] T. Nakamura, N. Fukuda, T. Kobayashi, N. Aoi, H. Iwasaki, T. Kubo, A. Mengoni, M. Notani, H. Otsu,

H. Sakurai, S. Shimoura, T. Teranishi, Y. X. Watanabe, K. Yoneda, and M. Ishihara, (1999) Coulomb Dissociation of ^{19}C and its Halo Structure, *Phys. Rev. Lett.* 83, 1112-1115.

[11] A.H. Wapstra, G. Audi and C. Thibault, (2003) The A_{ME} 2003 atomic mass evaluation (I). Evaluation of input data, adjustment procedures, *Nucl. Phys.* A 729, 129-336.

[12] K. Tanaka, T. Yamaguchi, T. Suzuki, T. Ohtsubo, M .Fukuda, D .Nishimura, M .Takechi, K .Ogata, A .Ozawa, T. Izumikawa, T. Aiba, N. Aoi, H.Baba, Y .Hashizume, K. Inafuku, N. Iwasa, K. Kobayashi, M. Komuro, Y. Kondo, T. Kubo, M. Kurokawa, T. Matsuyama, S. Michimasa, T. Motobayashi, T .Nakabayashi, S. Nakajima, T. Nakamura, H .Sakurai, R. Shinoda, M. Shinohara, H. Suzuki, E. Takeshita, S. Takeuchi, Y .Togano, K .Yamada, T. Yasuno, M. Yoshitake, (2010) Observation of a Large Reaction Cross Section in the Drip-Line Nucleus 22C, *Phys. Rev. Lett.* 104, 062701 .

[13] M.K. Sharma, A. Bhagwat, Z. A. Khan, W. Haider, and Y. K. Gambhir, (2011) Neutron density distribution and the halo structure of ^{22}C, *Phys. Rev.* C 83, 031601(R).

[14] M. El-Azab Farid, A. A. Ibraheem, J. H. Al-Zahrani, W. R. Al-Harbi and M. A. Hassanain, (2013) Alpha-deuteron (triton) analysis of 6(7) Li elastic Scattering, *J. Phys. G, Nucl. Part. Phys* 40, 075108.

[15] M. Aygun, Y. Kucuk, I. Boztosun and A. A. Ibraheem, (2010) Microscopic few-body and Gaussian-shaped density distributions for the analysis of the ^{6}He exotic nucleus with different target nuclei, *Nucl. Phys.* A 848, 245-259.

[16] F. Malaguti, A. Uguzzoni, E. Verondini and P. E. Hodgson, (1981) Nuclear charge Distributions, *Riv. Nuovo Cimento* 5(1), 326-392.

[17] P. E. Hodgson, (2005), Nuclear Charge and Matter Distributions, *Heavy-Ion Collisions* 168, 70-96.

[18] S. Ahmad, A. A. Usmani, Shakeb Ahmad, and Z. A. Khan, (2017) Interaction cross sections and matter radii of oxygen isotopes using the Glauber model, *Phys. Rev.* C 95, 054601.

[19] S. Ahmad, D. Chauhan, A.A. Usmani, Z.A. Khan, (2016) Study of the neon interaction cross section using the Glauber model, *Eur. Phys. J.* A 52, 128.

[20] M. Ismail, A. Y. Ellithi, and H. Abou-Shady, (2005) Effect of finite range of the NN force and NN cross section on reaction cross section for neutron rich nuclei, *Phys. Rev.* C 71, 027601.

[21] M. K. Sharma, R.N. Panda, M.K. Sharma, and S.K. Patra, (2015) Study of Reaction Cross Section of Light Mass Nuclei Using Glauber Formalisms, *Braz. J. Phys.* 45, 138-146.

[22] B. Abu-Ibrahim, W. Horiuchi, A. Kohama, and Y. Suzuki, (2008) Reaction cross sections of carbon isotopes incident on a proton,, *Phys. Rev.* C 77, 034607.

[23] X.Z. Cai, J.Feng , W .Shen, Ma Yugang, J.Wang , and Ye Wei, (1998) In-medium nucleon-nucleon cross section and its effect on total nuclear reaction cross section, *Phys. Rev.* C 58, 572-575.

[24] G.F. Bertsch and S. Das Gupta, (1988) A guide to microscopic models for intermediate energy heavy ion collisions, *Phys. Rep.* 160, 189-233.

[25] Y. Yuan, Q. Li, Zh. Li, and Fu-Hu Liu, (2010) Transport model study of nuclear stopping in heavy-ion collisions over the energy range from 0.09A to 160A GeV, *Phys. Rev.* C 81, 034913.

[26] C.A. Bertulani and C. De Conti, (2010) Pauli blocking and medium effects in nucleon knockout reactions, *Phys. Rev.* C 81, 064603.

[27] F. Sammarruca and P. Krastev, (2006) Effective nucleon-nucleon cross sections in symmetric and asymmetric nuclear matter, *Phys. Rev.* C 73, 014001.

[28] Y.X. Zhang, Zh. Li, and P. Danielewicz, (2007) In-medium NN cross sections determined from the nuclear stopping and collective flow in heavy-ion collisions at intermediate energies, *Phys. Rev.* C 75, 034615.

[29] V. Franco and Y. Yin, (1985) Elastic Scattering of α Particles and the Phase of the Nucleon-Nucleon Scattering Amplitude, *Phys. Rev. Lett.* 55, 1059-1061.

[30] D. Chauhan and Z. A. Khan, (2007) Unitary correlation operator method from a similarity renormalization group perspective, *Phys. Rev.* C 75, 054614.

[31] HAN Rui, CHEN Zhi-Qiang, R. Wada, ZHANG Su-Ya-La-Tu, LIU Xing-Quan, LIN Wei-Ping, JIN Zeng-Xue, HU Bi-Tao (2013) Effects of In-Medium Nucleon-Nucleon Cross Section and Nuclear Density Distribution on the Proton-Nucleus Total Reaction Cross Section, *CHIN. PHYS. LETT.* 30(12), 122501.

[32] D. Chauhan and Z. A. Khan, (2009) α-nucleus elastic scattering in the energy range 25-70 MeV/nucleon,

Eur. Phys. J. A 41, 179-188.

[33] L. Ray, (1979) Proton-nucleus total cross sections in the intermediate energy range, Phys. Rev. C 20, 1857-1872.

[34] S. Ahmad, A.A. Usmani and Z.A. Khan, (2017) Matter radii of light proton-rich and neutron-rich nuclear isotopes, Phys. Rev. C 96, 064602.

[35] M. Takechi, M. Fukuda, M. Mihara, K. Tanaka, T. Chinda, T. Matsumasa, M. Nishimoto, R. Matsumiya, Y. Nakashima, H. Matsubara, K. Matsuta, T. Minamisono, T. Ohtsubo, T. Izumikawa, S. Momota, T. Suzuki, T. Yamaguchi, R. Koyama, W. Shinozaki, M. Takahashi, A. Takizawa, T. Matsuyama, S. Nakajima, K. Kobayashi, M. Hosoi, T. Suda, M. Sasaki, S. Sato, M. Kanazawa, and A. Kitagawaal, (2009) Reaction cross sections at intermediate energies and Fermi-motion effect, Phys. Rev. C 79, 061601(R).

[36] S. Kox, A. Gamp, C. Perrin, J. Arvieux, R. Bertholet, J.F. Bruandet, M. Buenerd, Y. El Masri, N. Longequeue, F. Merchez, (1985) Transparency effects in heavy-ion collisions over the energy range 100–300 MeV/nucleon, Phys. Lett. B 159, 15-18.

[37] A. Ozawa, O. Bochkarev, L. Chulkov, D. Cortina, H. Geissel, M. Hellström, M. Ivanov, R. Janik, K. Kim ura, T. Kobayashi f, A.A. Korsheninnikov a, G. Mün zenberg b, F. Nickel b, Y. Ogawa g, A.A. Ogloblin, M. Pfützner, V. Pribora, H. Simon, B. Sitár, P. Strme n K. Yoshida, (2001) Measurements of interaction cross sections for light neutron-rich nuclei at relativistic energies and determination of effective matter radii, Nucl. Phys. A 691, 599-617.

[38] I. Tanihata, T. Kobayashi, O. Yamakawa, S. Shimour a 1, K. Ekuni 1, K. Sugimoto, N. Takahashi, T. Shim oda, H. Sato, (1988) Measurement of interaction cross sections using isotope beams of Be and B and isospin dependence of the nuclear radii, Phys. Lett. B 206, 592-596 (1988).

[39] D. Chauhan, Z.A. Khan and A.A. Usmani, (2014) Interaction cross sections for neon isotopes in the Glauber model and the halo structure of 31Ne, Phys. Rev. C 90, 024603.

[40] E. Liatard, J. F. Bruandet, F. Glasser, S. Kox, Tsan Ung Chan, G. J. Costa, C. Heitz, Y. El Masri, F. Hanappe, R. Bimbot, D. Guillemaud-Mueller and A. C. Mueller (1990) Matter Distribution in Neutron-Rich Light Nuclei and Total Reaction Cross-Section, Europhys. Lett. 13, 401-404.

[41] H. DE VRIES, C. W. DE JAGER, and C. DE VRIES, (1987) Nuclear charge-density-distribution parameters from elastic electron scattering, ATOMIC DATA AND NUCLEAR DATA TABLES 36, 495-536.

[42] A. Ingemarsson, J. Nyberg, P.U. Renberg, O. Sundbe rg, R.F. Carlson, A.J. Cox, A. Auce, R. Johansson, G . Tibell, Dao T. Khoa, R.E. Warner, (2000) New results for reaction cross sections of intermediate energy α-particles on targets from ^{9}Be to ^{208}Pb, Nucl. Phys. A 676, 3-31.

[43] Felix Horst, Giulia Aricò, Kai-Thomas Brinkmann, Stephan Brons, Alfredo Ferrari, Thomas Haberer, Andrea Mairani, Katia Parodi, Claire-Anne Reidel, Uli Weber, Klemens Zink, and Christoph Schuy, (2019) Measurement of 4He charge- and mass-changing cross sections on H, C, O, and Si targets in the energy range 70–220 MeV/u for radiation transport calculations in ion-beam therapy, Phys. Rev. C 99, 014603 (2019).

[44] H.Y. Zhang, W.Q. Shen, Z.Z. Ren, Y.G. Ma, W.Z. Ji ang, Z.Y. Zhu, X.Z. Cai, D.Q. Fang, C. Zhong, L.P. Yu, Y.B. Wei, W.L. Zhan, Z.Y. Guo, G.Q. Xiao, J.S. Wang, J.C. Wang, Q.J. Wang, J.X. Li, M. Wang and Z.Q. Chen, (2002) Measurement of reaction cross section for proton-rich nuclei (A<30) at intermediate energies, Nucl. Phys. A 707, 303-324.

[45] G. W. Fan, M. Fukuda, D. Nishimura, X. L. Cai, S. Fukuda, I. Hachiuma, C. Ichikawa, T. Izumikawa, M. Kanazawa, A. Kitagawa, T. Kuboki, M. Lantz, M. Mihara, M. Nagashima, K. Namihira, Y. Ohkuma, T. Ohtsubo, Zhongzhou Ren, S. Sato, Z. Q. Shen, M. Sugiyama, S. Suzuki, T. Suzuki, M. Takechi, T. Yamaguchi, B. J. Xu, and W. Xu, (2014) Structure of 8Li from a reaction cross-section measurement, Phys. Rev. C 90, 044321.

[46] R.F. Carlson, (1996) Proton-Nucleus Total Reaction Cross Sections and Total Cross Sections Up to 1 GeV, Atomic Data and Nucl. Data Tables, 63, 93-116.